Investigation of Soft Foundations with Surface Reinforcement

H. OHTA
Associated Professor, Dept of Civil Engineering, Kyoto University
R. MOCHINAGA
Manager, Engineering Dept, Sapporo Construction Bureau, Japan Highway Public Cooperation
N. KURIHARA
Senior Engineer, Sapporo Construction Bureau, Japan Highway Public Cooperation

SUMMARY Transverse surface reinforcements at the bottom of embankments placed on very soft foundations are found to reduce the amount of deformation of the foundations and improve the bearing capacities through the elastic-plastic finite element analysis on an idealized model of soft foundation as well as on a field trial embankment.

1 INTRODUCTION

It is being found, through field tests to improve bearing capacities and rigidities of soft foundations loaded by embankments, that restrictions on lateral movements of the ground surface beneath the load (such restrictions caused by steel reinforcements at the bottom of the embankments or at the surface of the soft ground) can be effective in increasing the bearing capacity and decreasing the undrained settlement (due mainly to lateral flow of soft material beneath the load). This lateral reinforcement has been achieved by using either strips, nets, bars or beams of steel or chemical or natural materials such as nylon or glass fibers or bamboo-fascines; Kawakami et. al. (1967), Eide and Holmberg (1972).

The effect of this sort of transverse reinforcement at the bottom of an embankment will depend not only on the material properties of the soft foundation but also on the geometry of the cross section of the fill and the stratification of the soft materials, especially on the ratio of the width of the embankment to the thickness of soft soil layer. This paper presents an investigation of the effectiveness of surface reinforcements, by the use of finite element computations on undrained behaviour and subsequent two dimensional consolidation deformation of loaded soft foundations with and without surface reinforcements, focusing on the width/thickness ratio while material properties are held constant throughout the investigation.

The constitutive equation employed in the finite element computations is an infinitesimal elastic-plastic stress-strain relation which is reduced to the Original Cam Clay model (Roscoe, Schofield and Thurairajah 1963) under conditions of isotropic initial stress state and which is able to describe the anisotropic behaviour of clay including the complicated responses to the rotation of principal stress directions as discussed by Sekiguchi and Ohta (1977) and by Ohta and Sekiguchi (1979).

2 CONSTITUTIVE EQUATION

2.1 Stress Parameters

It is convenient to introduce the stress parameters to appear in the following sections before discussing the details of the constitutive equation employed in the computations. The effective stress tensor σ'_{ij} is divided into two components; hydrostatic component p and deviatoric component s_{ij} where ij denotes (i,j) component of a tensor,

$$p=\frac{1}{3}\sigma'_{ij}\delta_{ij} \qquad (1) \qquad\qquad s_{ij}=\sigma'_{ij}-p\delta_{ij} \qquad (2)$$

δ_{ij} in Eqs.(1) and (2) is Kronecker's delta. In the Sekiguchi-Ohta model a new parameter "pressure-normalized deviatoric stress tensor η_{ij} is employed,

$$\eta_{ij}=\frac{s_{ij}}{p} \qquad (3)$$

The pressure-normalized deviatotric stress tensor at the end of Ko-consolidation is defined as

$$\eta_{ijo}=\frac{s_{ijo}}{p_o} \qquad (4)$$

where s_{ijo} and p_o are deviatoric stress and hydrostatic effective stress at the end of consolidation. The ratio of shear stress to hydrostatic effective stress can be defined in terms of pressure-normalized deviatoric stress tensor as

$$\eta^*=\sqrt{\frac{3}{2}(\eta_{ij}-\eta_{ijo})(\eta_{ij}-\eta_{ijo})} \qquad (5)$$

2.2 Material Constants

The material constants used in the Sekiguchi-Ohta model are introduced here,

1. λ and κ: parameters representing compressibility of soil respectively defined as 0.434Cc and 0.434Cs where Cc and Cs are compression and swelling indices,
2. D: parameter representing dilatancy of soil defined by Shibata (1963). In the Original Cam Clay model a parameter M is used (instead of D) which is related to D through

$$M=\frac{\lambda-\kappa}{D(1+e_o)} \qquad (6)$$

3. e_o: void ratio of soil isotropically or anisotropically consolidated with pressure of p_o. In the Original Cam Clay model p_o is taken as a unit value of pressure. However this discrepancy in the definition of p_o and hence of e_o is not essential.

2.3 Plastic Potential Function

The plastic potential function f assumed in the Sekiguchi-Ohta model is defined as

$$f=\frac{\lambda-\kappa}{1+e_o}\ln\frac{p}{p_o}+D\eta^*-v^p \qquad (7)$$

where hardening parameter v^p is the plastic volumetric strain. It may be appropriate to note that the yielding should occur when the principal stress directions rotate while both the effective hydro-

static pressure and the octahedral shear stress are kept fixed at the values of those at the end of Ko-consolidation, according to the Sekiguchi-Ohta model, because the value of stress ratio parameter η^* can increase by the rotation of principal stress directions. This does not mean that the model has lack of frame indifference, however, since the stress ratio parameter η^* is a scalar.

2.4 Stress-Strain Matrix (General)

The stress-strain matrix used in solving elastic-plastic problems by means of finite element method is derived here employing a technique proposed by Yamada, Yoshimura and Sakurai (1968). The elastic part of the stress-strain relation can be written in an incremental form as

$$d\sigma'_{ij} = D^e_{ijkl}(d\epsilon_{kl} - d\epsilon^p_{kl}) \tag{8}$$

where D^e_{ijkl} is the elastic stress-strain matrix and ϵ_{kl}, ϵ^p_{kl} are the total strain tensor and its plastic component respectively. The plastic component of strain increment is given as

$$d\epsilon^p_{ij} = \Lambda \frac{\partial f}{\partial \sigma'_{ij}} \tag{9}$$

where plastic potential function f is a function of the effective stress tensor and of hardening parameter L, i.e.

$$df = \frac{\partial f}{\partial \sigma'_{ij}} d\sigma'_{ij} + \frac{\partial f}{\partial L}\frac{\partial L}{\partial \epsilon^p_{ij}} d\epsilon^p_{ij} \tag{10}$$

A proportional function Λ is given by substituting Eqs.(8) and (9) into Eq.(10) as follows,

$$\Lambda = \frac{f_{ij} D^e_{ijkl} d\epsilon_{kl}}{\left(f_{ij} D^e_{ijkl} - \frac{\partial f}{\partial L}\frac{\partial L}{\partial \epsilon^p_{kl}}\right) f_{kl}} \tag{11}$$

where

$$f_{ij} = \frac{\partial f}{\partial \sigma'_{ij}}$$

Substituting Eqs.(9) and (11) into Eq.(8), we get a general form of the elastic-plastic stress-strain matrix as

$$d\sigma'_{ij} = (D^e_{ijop} - D^p_{ijop}) d\epsilon_{op} \tag{12}$$

where

$$D^p_{ijop} = D^e_{ijop} \frac{f_{mn} D^e_{mnop} f_{kl}}{\left(f_{mn} D^e_{mnqr} - \frac{\partial f}{\partial L}\frac{\partial L}{\partial \epsilon^p_{qr}}\right) f_{qr}} \tag{13}$$

If we adopt an incrementally linear isotropic elasticity in the elastic stress-strain matrix, we get

$$D^e_{ijop} = \bar{\lambda}\delta_{ij}\delta_{op} + \bar{\mu}(\delta_{io}\delta_{jp} + \delta_{ip}\delta_{jo}) \tag{14}$$

where $\bar{\lambda}$ and $\bar{\mu}$ are Lame's constants. Substituting the thus obtained Eq.(14) into Eq.(13), the plastic stress-strain matrix is reduced to

$$D^p_{ijop} = \frac{A_{ijop}}{B - C} \tag{15}$$

where

$$A_{ijop} = \bar{\lambda}^2 f_{kk}^2 \delta_{ij}\delta_{op} + 2\bar{\lambda}\bar{\mu} f_{kk}(f_{ij}\delta_{op} + f_{op}\delta_{ij}) + 4\bar{\mu}^2 f_{ij} f_{op} \tag{16}$$

$$B = \bar{\lambda} f_{mm} f_{qq} + 2\bar{\mu} f_{qr} f_{qr} \tag{17}$$

$$C = \frac{\partial f}{\partial L}\frac{\partial L}{\partial \epsilon^p_{qr}} f_{qr} \tag{18}$$

2.5 Stress-Strain Matrix (Sekiguchi-Ohta model)

The plastic stress-strain matrix can be specified through Eqs.(15)-(18) by calculating both f_{ij} which appears in these equations and C in Eq.(18). Differentiating the plastic potential function given by Eq.(7), we get

$$f_{ij} = \frac{D}{3p}\left(\frac{\lambda - K}{(1+e_0)D} - \frac{3}{2\eta^*}\frac{s_{kl}}{p}(\eta_{kl} - \eta_{klo})\right)\delta_{ij} + \frac{3D}{2\eta^* p}(\eta_{ij} - \eta_{ijo}) \tag{19}$$

$$C = -f_{qq} \tag{20}$$

By the use of Eqs.(19) and (20) we can specify all the components of the plastic stress-strain matrix.

3 FINITE ELEMENT COMPUTATIONS

3.1 Computer Programme

The computer programme employed in this investigation is the one originally written by Akai and Tamura (1976) for the model proposed by Ohta (1971) and Ohta, Yoshitani and Hata (1975) and afterwards modified by Tamura for the Sekiguchi-Ohta model which is employed in this investigation. Finite element formulation used in the Akai-Tamura programme is developed by adopting the technique proposed by Christian (1968) and Christian and Boehmer (1970). Although Christian used the forward finite difference scheme in his analysis of consolidation processes, the Akai-Tamura programme emp'oys the backward finite difference scheme so as t ensure better stability in computations.

3.2 Models Analysed

Imaginary embankments with and without the t ansverse reinforcement at the bottom of the fill placed on an imaginary uniform soft clay layer underlain by a very hard sand are analysed in order to estimate the effect of surface reinforcement on the deformability and the bearing capacity of soft clay foundation. The dimensions of the embankment are 20m in shoulder to shoulder distance and 40m in toe to toe distance. The weight of the embankment is chosen to be 100kN/m^2. The soft clay layer is assumed to be a slightly overconsolidated one which was consolidated under conditions of no lateral deformation with the vertical effective preconsolidation pressure σ'_{vo} of 90kN/m^2. The current effective overburden pressure σ'_{vi} is 75kN/m^2, i.e. the overconsolidation ratio is 1.2.

Analyses were carried out for 8 cases which are classified into two groups, one of which is without surface reinforcement and the other of which is the cases with reinforcement. Each group consists of 4 cases distinguished by the thickness H of the clay layer (H=5m, 10m, 15m, 20m) so that the effect of the ratio of the fill width and the thickness of soft layer is studied. It is generally estimated that the Young's modulus E of well compacted fill is between E=20,000kN/m^2-30,000kN/m^2. However in this investigation the rigidity of the fill itself is ignored for simplicity, i.e. the fill is substituted by a vertical load. The transverse reinforcement at the bottom of the embankment is replaced by an elastic band of 0.5m thickness, the elastic parameters of which are assumed to be E=1,000,000kN/m^2 and Poisson's ratio=0.3. Loading is incremental (20 steps) under fully undrained conditions and subsequent consolidation processes are computed stepwise through 40 steps.

The clay layer is assumed to be uniform, i.e., a particular set of material parameters and effective stress states both at the end of pre-consolidation and at the moment just before loading is assigned to the clay regardless of the depth. Although this assumption is not very realistic, it provides a simpler and clearer comparison between the performance

of reinforced fill and unreinforced fill placed on a thin clay layer as well as on a thick clay layer. The clay layer is assumed in this investigation to have been anisotropically (Ko=0.5) preconsolidated with the effective vertical stress of 90kN/m^2 (e_o= 1.5) and then have been brought to a slightly over-consolidated state with the current effective overburden pressure of 75kN/m^2 (coefficient of earth pressure at rest is assumed to remain at 0.5). The material parameters are λ=0.231, κ=0.042, D=0.053, permeability=5x10^{-5} m/day. During the consolidation process, the pore water is allowed to drain either from the surface or from the bottom of the soft clay layer.

3.3 Computed Results

Figs.1 (a) and (b) show the settlement of the surface of the clay layer beneath the centre of the embankment during undrained loading and the subsequent consolidation process for the case of unreinforced fill and of reinforced fill, respectively.

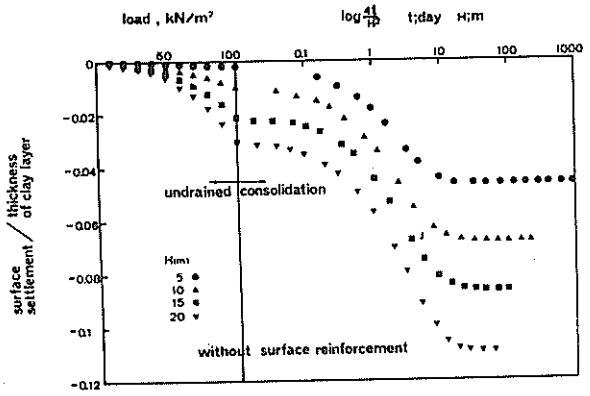

(a) Unreinforced fill

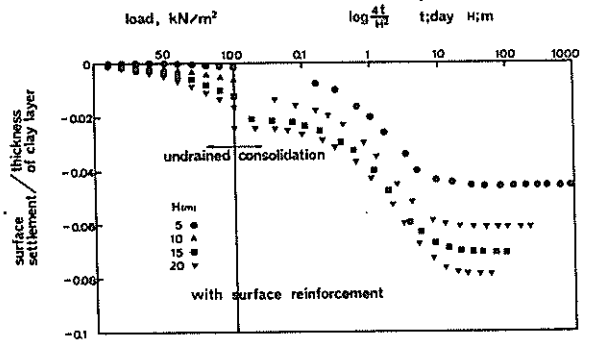

(b) Reinforced fill

Figure 1 Settlement at the centre of fill

From the above model and computations, it is found that the surface reinforcement reduces the settlement both for undrained and drained consolidation processes.

Figs.2 (a) and (b) show the overall patterns of surface settlement for both cases. It is also clear that the surface reinforcement reduces the settlement of the embankment and the heave of the ground surface adjacent to the embankment. It may be noteworthy that the settlement of the centre of the fill is much less than the settlement of the shoulder of the fill in the case of thin soft clay layer, especially for unreinforced fill.

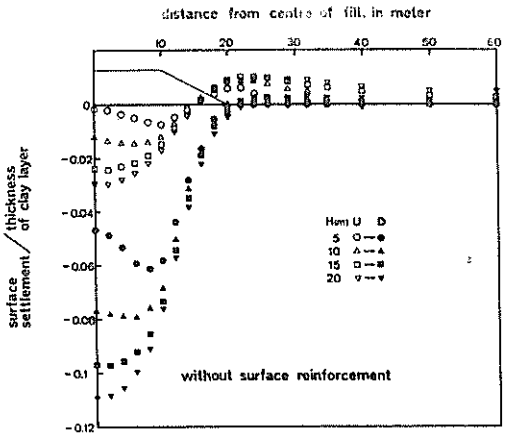

(a) Unreinforced fill

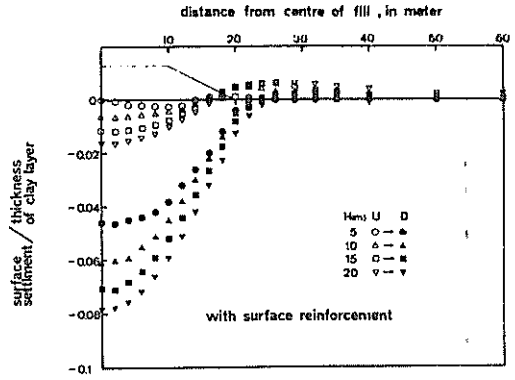

(b) Reinforced fill

Figure 2 Patterns of surface settlement at the end of undrained loading (U) and consolidation (D)

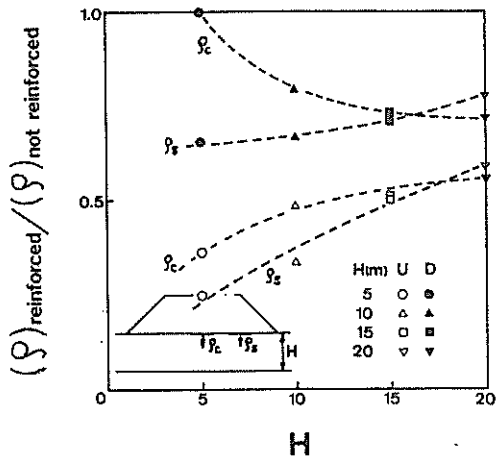

Figure 3 Settlement reduction effect of surface reinforcement

Summarizing the results shown in Figs.1 and 2, the settlement reduction effect of surface reinforcement can be roughly estimated through Fig.3 where the settlement reduction ratio is defined by the settlement of reinforced fill divided by the settlement of unreinforced fill. The surface settlements beneath the centre and beneath the shoulder of the fill are denoted by ρ_c and ρ_s respectively. Generally speaking, the surface reinforcement is more effective in reducing the undrained settlement, shown by white

marks plotted in Fig.3, below drained settlement (black marks). Fig.3 also shows the better performance of surface reinforcement in the case of thinner clay layer rather than in the case of thicker clay layer, both for undrained and drained settlement in general. The reduction of drained settlement caused by the surface reinforcement can be explained as the consequence of a smaller amount of volume decrease due to the dilatancy characteristics accompanied by distortional deformation of clay.

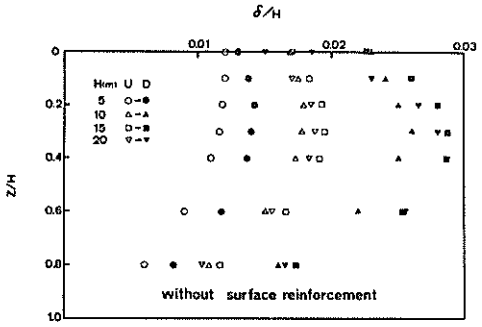

(a) Unreinforced fill

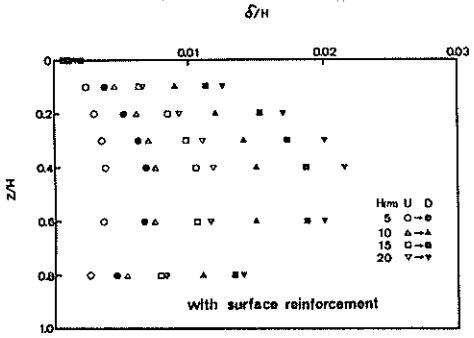

(b) Reinforced fill

Figure 4 Horizontal displacement beneath the toe of the embankment

The horizontal displacement of the points initially located on a vertical line beneath the toe of the fill are plotted in Figs.4 (a) and (b) showing that the surface reinforcement reduces the horizontal displacement not only at the surface of soft clay but also at any depth, both in the case of undrained loading and of fully drained.

All the Figs.1-4 suggest that the surface reinforcement is effective in reducing the amount of deformation of soft clay layer loaded by an embankment. However we are interested in estimating the effect of surface reinforcement on the bearing capacity of the soft foundation as well as its deformability. Unfortunately, the ultimate bearing capacity of a soft clay layer can hardly be estimated by finite element computations. In this investigation an indirect method of estimating the bearing capacity proposed by Matsuo and Kawamura (1974) is employed. Based on a great deal of data obtained from a number of trial embankments placed on various type of soft foundations, they found the existence of a very narrow band which they called the "failure criterion curve" on a diagram the ordinate of which was the settlement ρ of the ground surface at the centre of the fill and the abscissa of which was the horizontal displacement δ of the ground surface at the toe of the fill divided by ρ. According to them, it is a serious warning when ρ-δ/ρ plot measured during construction of a fill comes very near to the failure criterion curve. This warning may be only a crude guidance for possible failure of foundations, and the theoretical background of their proposal is still open to question. However, additional case studies carried by Matsuo and Kawamura (1977) and Matsuo, Kuroda, Asaoka and Kawamura (1977) show that their failure criterion curve gives a reasonable prediction of failure of an embankment for either rapid or very slow loading process.

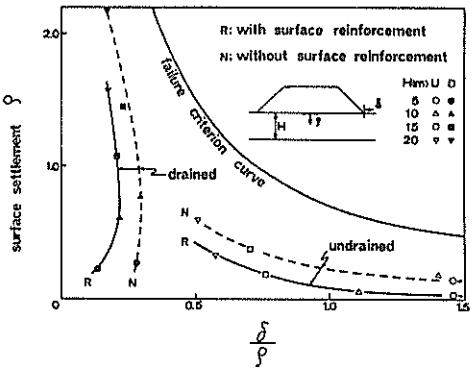

Figure 5 Foundation stabilizing effect of surface reinforcement

Fig.5 shows the stability estimations of the fill with and without surface reinforcement for either the undrained loading process or the fully drained state. In each case the plots for the reinforced embankment are located farther from the failure criterion curve in Fig.5 showing that the reinforced embankments are safer than the embankments without the reinforcement. The computed horizontal displacements at the toes of the reinforced embankments are very small as shown in Fig.4 (b) and consequently give very small values of δ/ρ. Plotting Fig.5, the horizontal displacement δ of the reinforced fill is calculated by multiplying the maximum value of horizontal displacement among those points located on the vertical line beneath the toe of the reinforced embankment by the ratio of the horizontal displacement at the surface of the ground to that at a depth where the largest horizontal displacement is induced for the unreinforced embankment. Thus obtained equivalent horizontal displacements at the toe of the embankment are plotted in Fig.5 showing a conservative estimate of the effect of the reinforcement on the increase in stability. Fig.5 does not give a quantitative increase in the factor of safety due to the surface reinforcement. However we see in Fig.5 a general tendency of the effectiveness of surface reinforcement.

Although the results discussed above are only computational results of an idealised model and not reality, we can still conclude that surface reinforcement is effective in reducing the deformation of soft foundation and in stabilising the embankment as well.

4 FIELD TRIAL EMBANKMENT

4.1 Trial Embankment at Ebetsu

A trial embankment was placed on a very soft layer of peat and clay at Ebetsu, Hokkaido in order to obtain data of settlement and of stability of a newly proposed motorway from Sapporo to Iwamizawa (32 km) about 85% of which was to be high embankment (5 -8m) on very soft layer of peat and clay (20-35m thick). The trial embankment, 386.3m long, was divided into 4 sections; natural ground section, surface reinforcement section with sand drain treatment, sand compaction pile section and chemical pile section, each of which was about 50m.

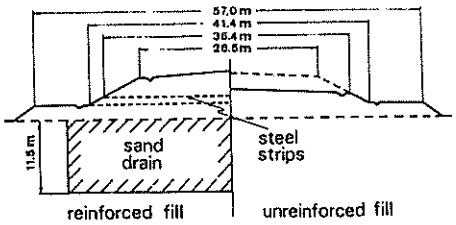

Figure 6 Cross sectional views of trial embankment

The cross sectional views of natural ground section and surface reinforcement section are shown in Fig. 6 where we see the sand drain treatment under the surface reinforcement section. These sections were to be loaded up to the fill height of about 8.5m above the original ground surface. The reinforced section was raised to the proposed height without having any cracks, but the natural ground section had a major crack (0.1m wide, 10m long) along the centre line of the fill accompanied by two minor cracks along the line joining the main body of the fill with the berm on both sides of the embankment when the fill height was about 3.5m above the original ground surface. After finding these cracks, the natural ground section was left without any additional loading while the other three sections underwent further loading.

Table I Parameters used in computation

type of soil	peat	clay with peat	sand	silty clay	sand	silty clay	sand	silty clay
depth m	0 - 3 0 - 4	3 - 6 4 - 6	6 - 7 6 - 8	7 - 9 8 -10	9 -11 10-11	11 -18	18-19	19 -30
λ	1.73	0.35	0.06	0.22	0.06	0.17	0.06	0.17
κ	0.17	0.13	0.02	0.12	0.02	0.06	0.01	0.06
D	0.11	0.08	0.02	0.06	0.02	0.05	0.02	0.05
σ'_{vo} kN/m^2	20	50	200	70	200 450	180	1170	180
e_o	7	1.6	0.8	1.2	0.8	1.1	0.7	1.1
K_o	0.6	0.6	0.6	0.6	0.6	0.6	0.6	0.6
σ'_{vi} kN/m^2	1	9 7	20	31 35	20 46	85 80	120 115	172 167
K_I	1.4	1.1	0.6	0.75	0.6	0.76	0.6	0.6
permeability $k_{m/day}$	6×10^{-3} 10^{-3}	4.2×10^{-3} 7×10^{-4}	21 3.5	6×10^{-3} 10^{-3}	21 3.5	7×10^{-4}	3.5	7×10^{-4}

upper column for reinforced fill; lower column for unreinforced fill

Because this example was considered somewhat extreme and perhaps unpresentative, it was decided to carry out an analysis employing the computer programme introduced in the previous section. The material parameters for peat and clay were determined as follows: (1) λ from Cc value obtained from oedometer tests, (2) M in Eq.(6), which is related to ϕ' value , is calculated from c_u/p value estimated in laboratory tests, (3) Cs/Cc is calculated from an empirical equation 1-Cs/Cc=M/1.75 proposed by Karube (1975). For sand we determined ϕ value from which M is obtained leading to the value of Cs/Cc through Karube's equation. Although the value of Cc or Cs was not obtained in the laboratory tests for sand, the value of λ was determined in a way the authors thought reasonable without having any objective justification. The sand layers were treated as if they were overconsolidated with an overconsolidation ratio of 10. The permeabilities of peat, clay and sand were assumed to be 10 times those obtained from oedometer tests or from permeability tests for natural ground and 60 times for the ground with sand drain treatment. All the parameters used in the computations are listed in Table I. The surface reinforcement was replaced by a 1.2m thick elastic band ($E=2.2\times10^5$ kN/m^2, Poisson's ratio=0.3).

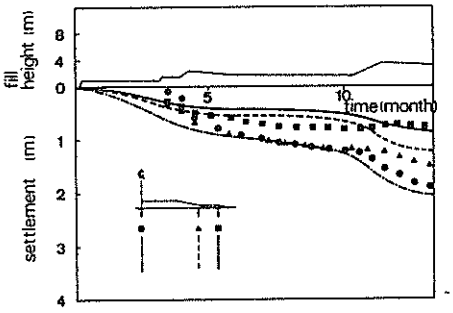

(a) Unreinforced section

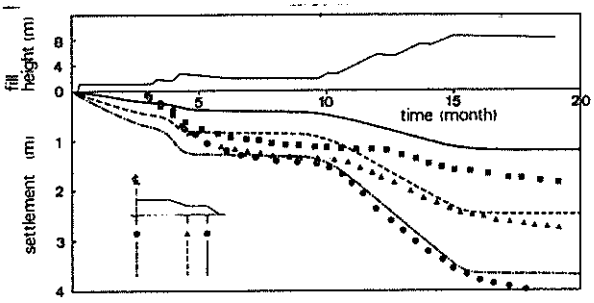

(b) Reinforced section

Figure 7 Settlement-time relations

Fig.7 shows the general tendency of the settlement-time relations both for the natural ground section and the surface reinforcement section. The computed curves roughly agree with measured settlements shown by the plots in Fig.7.

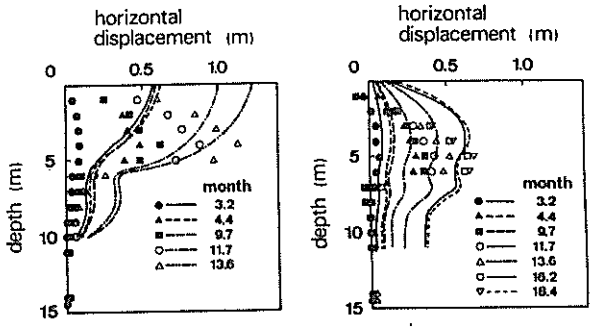

(a) Unreinforced section (b) Reinforced section

Figure 8 Horizontal displacement at the toe of embankment

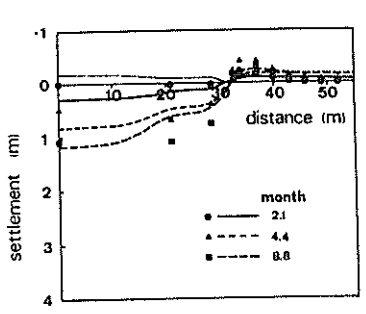

(a) Unreinforced section

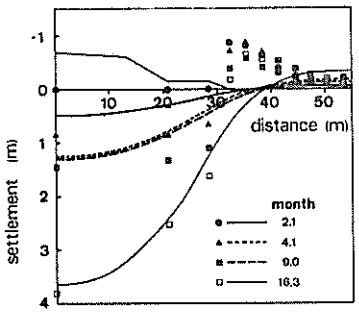

(b) Reinforced section
Figure 9 Surface settlement

Figs.8 and 9 show the general patterns of horizontal displacement of the points initially located on a vertical line beneath the toe of the fill and of the settlement of the ground surface (plots for measured and curves for computed). Because the fills are replaced by vertical loads in the computation the horizontal displacement near the surface of the ground in the case of unreinforced fill is computed to be larger than measured displacement. However it seems to the authors that the computed results are acceptable and that this acceptable performance of the computation gives some support to the discussions in the previous section derived from the same computer programme employed in the analysis presented in this section.

5 CONCLUSIONS

A finite element analysis of an idealized model suggests that the transverse surface reinforcement at the bottom of an embankment placed on a very soft foundation can considerably reduce the amount of deformation of the foundation and improve the bearing capacity. The performance of a field trial embankment demonstrating the effectiveness of surface reinforcement is introduced and back-analysed, with reasonable agreement, by means of a finite element technique exactly the same as the one employed in the analysis of the idealized model. As the result of these investigations, it is concluded that the transverse surface reinforcement is one possible technique to improve the undesirable characteristics of soft foundations.

6 ACKNOWLEDGEMENTS

It is acknowledged that the finite element computations reported in this paper were carried out using the FACOM M200 digital computer of the Computer centre, Kyoto University. Some of the studies described in this paper were supported by a grant (No. 3851 43, 1978-1979) from the Ministry of Education.

7 REFERENCES

AKAI, K. and TAMURA, T. (1976). An application of nonlinear stress-strain relations to multi-dimensional consolidation problems. Annuals, Disaster Prevention Research Institute, Kyoto Univ., No.19, B-2, pp 15-29, (in Japanese).

Christian, J.T. (1968). Undrained stress distribution by numerical method. Proc.A.S.C.E., SM 6, pp 1333-1345.

CHRISTIAN, J.T. and BOEHMER, J.W. (1970). Plane strain consolidation by finite elements. Proc.A.S.C.E., SM 4, pp 1435-1457.

EIDE, O. and HOLMBERG, S. (1972). Test fills to failure on the soft Bangkok clay. Proc. Specialty Conf. on Performance of Earth and Earth-Supported Structures, Vol.1, Part 1, pp 159-180.

KARUBE, D. (1975). Unstandardized triaxial testing procedures and related subjects for inquiry. Proc. 20th Symp. on Geotechnical Engineering, pp 45-60, (in Japanese).

KAWAKAMI, F., SATAKE, M., OGAWA, S., ITOH, T. and SATO, S. (1967). Stress measurement and analysis of H-shaped steel beam placed beneath a breakwater embankment in Ishinomaki Industrial Harbour. Journal of Japan Society for Soil MEch. and Found. Engrg, Vol.15, No.9, pp 15-19, (in Japanese).

MATSUO, M. and KAWAMURA, K. (1975). Study on modified method of design of embankment by observation during construction. Proc.J.S.C.E., No.240, pp 113-123, (in Japanese).

MATSUO, M. and KAWAMURA, K. (1977). Diagram for construction control of embankment on soft ground. Soils and Foundations, Vol.17, No.3, pp 37-52.

MATSUO, M., KURODA, K., ASAOKA, A. and KAWAMURA, K. (1977). Dynamic decision procedure of embankment construction. Proc. 9th Int. Conf. on S 'l Mech. Found. Engrg, Vol.2, pp 117-120.

OHTA, H. (1971). Analysis of deformations of soils based on the theory of plasticity and its application to settlement of embankments. Dr.Eng. Thesis submitted to Kyoto Univ.

OHTA, H., YOSHITANI, S. and HATA, S. (1975). Anisotropic stress-strain relationship of clay and its application to finite element analysis. Soils and Foundations, Vol. 15, No.4, pp 62-79.

OHTA, H. and SEKIGUCHI, H. (1979). Constitutive equations considering anisotropy and stress reorientation in clay. Proc. 3rd Int. Conf. on Numerical Methods in Geomechanics, Aachen, A.A.Balkema, Rotterdam, pp 475-484.

ROSCOE, K.H., SCHOFIELD, A.N. and THURAIRAJAH, A. (1963). Yielding of clays in states wetter than critical. Geotechnique, Vol.13, pp 211-240.

SEKIGUCHI, H. and OHTA, H. (1977). Induced anisotropy and time dependency in clays. Constitutive Equations of Soils, Proc. Specialty Session 9, Ninth Int. Conf. Soil Mech. Found. Engrg, Tokyo, pp 229-238.

SHIBATA, T. (1963). On the volume changes of normally-consolidated clays. Annuals, Disaster Prevention Research Institute, Kyoto Univ., No.6, pp 128-134, (in Japanese).

YAMADA, Y., YOSHIMURA, N. and SAKURAI, T. (1968). Plastic stress-strain matrix and its application for the solution of elastic-plastic problems by the finite element method. Int. J. Mech. Sci., Vol.10, pp 343-354.